

# Hadronic light-by-light scattering contribution to the muon $g - 2$ on the lattice

Andreas Nyffeler

PRISMA Cluster of Excellence, Institut für Kernphysik,  
Helmholtz-Institut Mainz  
Johannes Gutenberg Universität Mainz, Germany  
[nyffeler@uni-mainz.de](mailto:nyffeler@uni-mainz.de)



JOHANNES GUTENBERG  
UNIVERSITÄT MAINZ



Helmholtz-Institut Mainz



Workshop on Flavour changing and conserving processes 2017 (FCCP2017)  
Anacapri, Capri Island, Italy, 7-9 September 2017

## HLbL on the lattice: activities by Mainz group

Part I: Position-space approach to hadronic light-by-light scattering in the muon  $g - 2$  on the lattice

Nils Asmussen, Antoine Gérardin, Jeremy Green, Harvey Meyer, AN

Idea first presented in talks by Asmussen at meeting of German Physical Society (DPG), Heidelberg, March 2015 and by Green at Lattice 2015 (arXiv:1510.08384).

More details in talks by Asmussen at Lattice 2016 (arXiv:1609.08454), Lattice 2017 and by Meyer at “Muon  $g - 2$  Theory Initiative” Workshop near Fermilab 2017. Work in preparation.

Part II: Lattice calculation of the pion transition form factor  $\pi^0 \rightarrow \gamma^* \gamma^*$

Antoine Gérardin, Harvey Meyer, AN

Phys. Rev. D94, 074507 (2016)

Part III: Light-by-light forward scattering amplitudes in lattice QCD

Antoine Gérardin, Jeremy Green, Oleksii Gryniuk, Georg von Hippel, Harvey Meyer, Vladimir Pascalutsa, Hartmut Wittig

Phys. Rev. Lett. 115, 222003 (2015)

Talk by Gérardin at Lattice 2017

## State of the art for HLbL in the muon $g - 2$

- Not fully related to experimental cross sections
- Until now only model dependent estimates of total contribution
- → Large model uncertainties
- Uncertainties need to be reduced and better controlled to fully profit from future muon  $g - 2$  experiments at Fermilab and J-PARC
- Phenomenology

Use dispersion relations to reduce model uncertainties for dominant contributions using experimental input from

$$\gamma^* \gamma^{(*)} \rightarrow \pi^0, \eta, \eta'; \pi^+ \pi^-, \pi^0 \pi^0 \text{ (still to be measured !)}$$

Try to reconstruct input for DR from other hadronic processes.

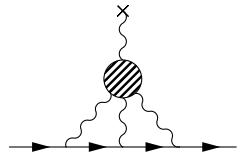
Colangelo *et al.* '14, '15, '17

Pauk and Vanderhaeghen '14

- Lattice QCD

Can provide a model independent first-principle estimate.

*Only publications from essentially one group so far: Blum *et al.* (RBC-UKQCD) '05, ..., '15, '16, '17*



# HLbL in muon $g - 2$ from Lattice QCD: Mainz approach

Developed independently from RBC-UKQCD

(Asmussen, Green, Meyer, AN '15 – '17)

- QCD blob: lattice regularization
- Everything else: position-space perturbation theory in Euclidean formulation

Similarities to approach by RBC-UKQCD '15, '16, '17:

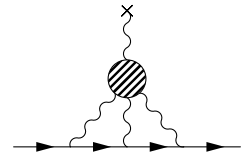
- Position-space (most natural for lattice QCD)
- Perturbative treatment of the QED part
- Get directly  $a_\mu^{\text{HLbL}} = F_2(k^2 = 0)$  as spatial moment

Strengths of our approach:

- Semi-analytical calculation
- QED part computed in continuum and in infinite volume
- Lorentz covariance manifest
- No power law effects  $1/L^2$  in the volume

Challenges:

- Need to calculate a QCD four-point function on the lattice
- Numerical efficiency not yet shown



Focus in this talk on semi-analytical calculation of perturbative QED part.

## HLbL in muon $g - 2$ in position-space

Project on anomalous magnetic moment (Euclidean space):

$$a_\mu^{\text{HLbL}} = F_2(0) = \frac{-i}{48m} \text{Tr}\{[\gamma_\rho, \gamma_\sigma](-i\cancel{p} + m)\Gamma_{\rho\sigma}(p, p)(-i\cancel{p} + m)\}$$

with on-shell muon momentum  $p = im\hat{\epsilon}$  ( $p^2 = -m^2$ ;  $\hat{\epsilon}$ : unit vector).

Vertex function in terms of position-space functions:

$$\Gamma_{\rho\sigma}(p, p) = -e^6 \int_{x,y} K_{\mu\nu\lambda}(x, y, p) \hat{\Pi}_{\rho;\mu\nu\lambda\sigma}(x, y)$$

$$K_{\mu\nu\lambda}(x, y, p) = \gamma_\mu(i\cancel{p} + \cancel{\partial}^{(x)} - m)\gamma_\nu(i\cancel{p} + \cancel{\partial}^{(x)} + \cancel{\partial}^{(y)} - m)\gamma_\lambda \mathcal{I}(\hat{\epsilon}, x, y)$$

$$\mathcal{I}(\hat{\epsilon}, x, y) = \int_{q,k,\text{IR-reg}} \frac{1}{q^2 k^2 (q+k)^2} \frac{1}{(p-q)^2 + m^2} \frac{1}{(p-q-k)^2 + m^2} e^{-i(q \cdot x + k \cdot y)}$$

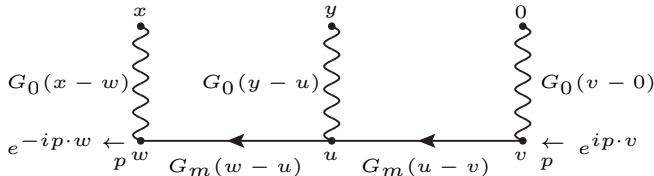
$$\hat{\Pi}_{\rho;\mu\nu\lambda\sigma}(x, y) = \int_z i z_\rho \langle j_\mu(x) j_\nu(y) j_\sigma(z) j_\lambda(0) \rangle$$

- $\mathcal{I}$  is logarithmically infrared divergent for  $p^2 = -m^2$   
⇒ introduce IR regulator.
- In  $a_\mu^{\text{HLbL}}$  only terms with derivatives remain and  $K_{\mu\nu\lambda}$  is infrared finite.

Notation:  $\int_q \equiv \int \frac{d^4 q}{(2\pi)^4}$ ,  $\int_x \equiv \int d^4 x$

## Evaluating $\mathcal{I}(\hat{\epsilon}, x, y)$

Diagrammatic representation of  $\mathcal{I}(\hat{\epsilon}, x, y)$ :



$$\mathcal{I}(\hat{\epsilon}, x, y) = \int_{u, \text{IR-reg}} G_0(u - y) J(\hat{\epsilon}, u) J(\hat{\epsilon}, x - u)$$

$$J(\hat{\epsilon}, u) = \int_v G_0(v + u) e^{-m\hat{\epsilon} \cdot v} G_m(v) = \sum_{n \geq 0} z_n(u^2) U_n(\hat{\epsilon} \cdot \hat{u})$$

Last expression: expansion in terms of Chebyshev polynomials of the second kind  $U_n$  (special case of the Gegenbauer polynomials)

$z_n$ : linear combination of products of two modified Bessel functions  $K_m$  and  $I_k$

Propagators in position-space:

$$G_0(x) = \frac{1}{4\pi^2 x^2}$$

$$G_m(x) = \frac{m}{4\pi^2 |x|} K_1(m|x|) \quad (K_1 \text{ is a modified Bessel function})$$

Averaging over direction of muon momentum  $p = im\hat{e}$

Evaluating Dirac trace in projector, one obtains an expression of the form

$$a_\mu^{\text{HLbL}} = \frac{me^6}{3} \int_y \int_x \mathcal{L}_{[\rho,\sigma];\mu\nu\lambda}(\hat{e}, x, y) i\hat{\Pi}_{\rho;\mu\nu\lambda\sigma}(x, y)$$

Exploit invariance of  $a_\mu$  under  $O(4)$  rotations of the muon momentum and average kernel  $\mathcal{L}$  over direction  $\hat{e}$  (Barbieri + Remiddi '75)

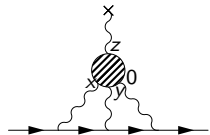
$$\bar{\mathcal{L}}_{[\rho,\sigma];\mu\nu\lambda}(x, y) = \frac{1}{2\pi^2} \int d\Omega_{\hat{e}} \mathcal{L}_{[\rho,\sigma];\mu\nu\lambda}(\hat{e}, x, y) \equiv \langle \mathcal{L}_{[\rho,\sigma];\mu\nu\lambda}(\hat{e}, x, y) \rangle_{\hat{e}}$$

Angular average can be performed analytically by using orthogonality property of Chebyshev (Gegenbauer) polynomials that appear in QED kernel  $\mathcal{L}$  via  $\mathcal{I}$  and  $J$  (hyperspherical approach):

$$\langle U_n(\hat{e} \cdot \hat{x}) U_m(\hat{e} \cdot \hat{y}) \rangle_{\hat{e}} = \frac{\delta_{nm}}{n+1} U_n(\hat{x} \cdot \hat{y})$$

## HLbL master formula in position-space

$$a_\mu^{\text{HLbL}} = \frac{me^6}{3} \int d^4y \int d^4x \underbrace{\bar{\mathcal{L}}_{[\rho,\sigma];\mu\nu\lambda}(x,y)}_{\text{QED}} \underbrace{i\hat{\Pi}_{\rho;\mu\nu\lambda\sigma}(x,y)}_{\text{QCD}}$$



After contracting the Lorentz indices the integration reduces to a 3-dimensional integral over  $x^2, y^2, x \cdot y$ .

QCD four-point function

$$i\hat{\Pi}_{\rho;\mu\nu\lambda\sigma}(x,y) = - \int d^4z z_\rho \langle j_\mu(x)j_\nu(y)j_\sigma(z)j_\lambda(0) \rangle$$

QED kernel function  $\bar{\mathcal{L}}_{[\rho,\sigma];\mu\nu\lambda}(x,y)$

- Weights the QCD four-point function in position-space.
- Tensor decomposition leads to 6 weight functions (and derivatives thereof) that depend on the 3 variables  $x^2, y^2, x \cdot y$ .
- We have computed these weight functions on a grid to about 5 digits precision, once and for all, and stored on disk.

## Tensor decomposition of QED kernel and weight functions

$$\bar{\mathcal{L}}_{[\rho,\sigma]:\mu\nu\lambda}(x,y) = \sum_{A=I,II,III} \mathcal{G}_{\delta\rho\sigma\mu\alpha\nu\beta\lambda}^A T_{\alpha\beta\delta}^A(x,y)$$

$\mathcal{G}_{\delta\rho\sigma\mu\alpha\nu\beta\lambda}^{I,II,III}$  = sums of products of Kronecker deltas (from Dirac trace)

$$T_{\alpha\beta\delta}^I(x,y) = \partial_\alpha^{(x)} (\partial_\beta^{(x)} + \partial_\beta^{(y)}) V_\delta(x,y)$$

$$T_{\alpha\beta\delta}^{II}(x,y) = m \partial_\alpha^{(x)} (T_{\beta\delta}(x,y) + \frac{1}{4} \delta_{\beta\delta} S(x,y))$$

$$T_{\alpha\beta\delta}^{III}(x,y) = m (\partial_\beta^{(x)} + \partial_\beta^{(y)}) (T_{\alpha\delta}(x,y) + \frac{1}{4} \delta_{\alpha\delta} S(x,y))$$

Scalar:  $S(x,y) = \langle \mathcal{I} \rangle_{\hat{\epsilon}}$  (IR regulated)

Vector:  $V_\delta(x,y) = \langle \hat{\epsilon}_\delta \mathcal{I} \rangle_{\hat{\epsilon}}$

Tensor:  $T_{\beta\delta}(x,y) = \langle (\hat{\epsilon}_\beta \hat{\epsilon}_\delta - \frac{1}{4} \delta_{\beta\delta}) \mathcal{I} \rangle_{\hat{\epsilon}}$

$$S(x,y) = g^{(0)}$$

$$V_\delta(x,y) = x_\delta g^{(1)} + y_\delta g^{(2)}$$

$$T_{\alpha\beta}(x,y) = (x_\alpha x_\beta - \frac{x^2}{4} \delta_{\alpha\beta}) I^{(1)} + (y_\alpha y_\beta - \frac{y^2}{4} \delta_{\alpha\beta}) I^{(2)} + (x_\alpha y_\beta + y_\alpha x_\beta - \frac{x \cdot y}{2} \delta_{\alpha\beta}) I^{(3)}$$

where the 6 weight functions depend on  $x^2, y^2, x \cdot y$ .

Example: Weight function  $g^{(2)}(x^2, x \cdot y, y^2)$

$$\begin{aligned}
g^{(2)}(x^2, x \cdot y, y^2) &= \frac{1}{8\pi y^2 |x| \sin^3 \beta} \int_0^\infty du u^2 \int_0^\pi d\phi_1 \\
&\times \left[ 2 \sin \beta + \left( \frac{y^2 + u^2}{2|u||y|} - \cos \beta \cos \phi_1 \right) \frac{\log \chi}{\sin \phi_1} \right] \\
&\times \sum_{n=0}^{\infty} \left\{ z_n(|u|) z_{n+1}(|x - u|) \left[ |x - u| \cos \phi_1 \frac{U_n}{n+1} + (|u| \cos \phi_1 - |x|) \frac{U_{n+1}}{n+2} \right] \right. \\
&\quad \left. + z_{n+1}(|u|) z_n(|x - u|) \left[ (|u| \cos \phi_1 - |x|) \frac{U_n}{n+1} + |x - u| \cos \phi_1 \frac{U_{n+1}}{n+2} \right] \right\}
\end{aligned}$$

where

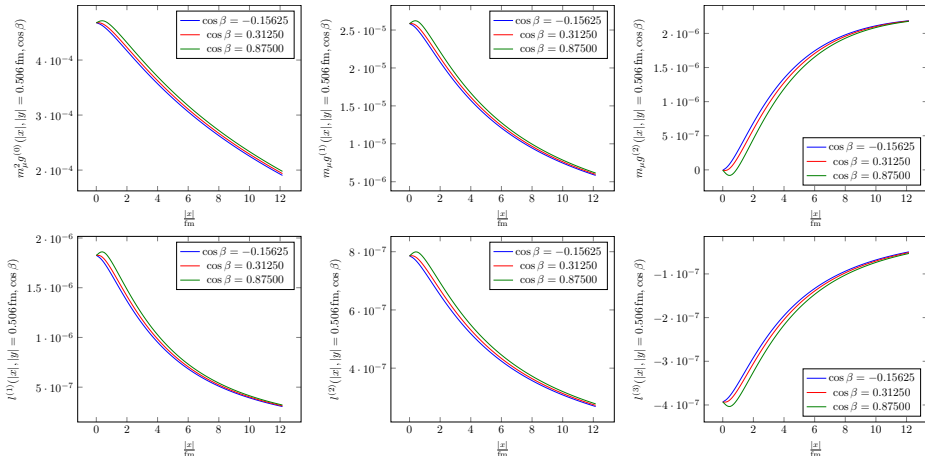
$$x \cdot y = |x||y| \cos \beta, \quad |x - u| = \sqrt{|x|^2 + |u|^2 - 2|x||u| \cos \phi_1}$$

$$\chi = \frac{y^2 + u^2 - 2|u||y| \cos(\beta - \phi_1)}{y^2 + u^2 - 2|u||y| \cos(\beta + \phi_1)}, \quad U_n = U_n \left( \frac{|x| \cos \phi_1 - |u|}{|u - x|} \right)$$

$z_n$  = linear combination of products of two modified Bessel functions.

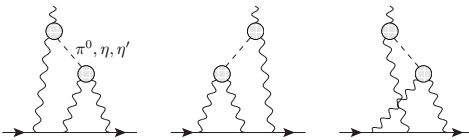
# Weight functions: $|x|$ dependence

For  $|y| = 0.506$  fm:



$g^{(0)}(|x|, x \cdot y, |y|)$  contains an arbitrary additive constant (due to the IR divergence in  $\mathcal{I}(\hat{\epsilon}, x, y)$ ), which does not contribute to  $\bar{\mathcal{L}}_{[\rho, \sigma]; \mu\nu\lambda}(x, y)$ .

# Numerical tests of QED kernel: (I) Pion-pole contribution to $a_\mu^{\text{HLbL}}$



Vector-meson dominance (VMD) model for illustration

Pion transition form factor in momentum space:

$$\mathcal{F}_{\pi^0 \gamma^* \gamma^*}(-q_1^2, -q_2^2) = \frac{c_\pi}{(q_1^2 + m_V^2)(q_2^2 + m_V^2)}, \quad c_\pi = -\frac{N_c m_V^4}{12\pi^2 F_\pi}$$

Parameters in pion-pole contribution:  $m_V$ , normalization  $1/F_\pi$  and  $m_\pi$  from pion propagator.

HLbL tensor in position-space (convolution):

$$i\hat{\Pi}_{\rho;\mu\nu\lambda\sigma}(x, y) = \frac{c_\pi^2}{m_V^2(m_V^2 - m_\pi^2)} \frac{\partial}{\partial x_\alpha} \frac{\partial}{\partial y_\beta} \left\{ \epsilon_{\mu\nu\alpha\beta} \epsilon_{\sigma\lambda\rho\gamma} \left( \frac{\partial}{\partial x_\gamma} + \frac{\partial}{\partial y_\gamma} \right) K_\pi(x, y) \right. \\ \left. + \epsilon_{\mu\lambda\alpha\beta} \epsilon_{\nu\sigma\gamma\rho} \frac{\partial}{\partial y_\gamma} K_\pi(y - x, y) + \epsilon_{\mu\sigma\alpha\rho} \epsilon_{\nu\lambda\beta\gamma} \frac{\partial}{\partial x_\gamma} K_\pi(x, x - y) \right\}$$

where

$$K_\pi(x, y) \equiv \int d^4 u \left( G_{m_\pi}(u) - G_{m_V}(u) \right) G_{m_V}(x - u) G_{m_V}(y - u) = K_\pi(y, x)$$

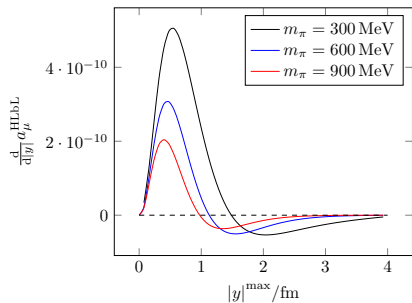
# Numerical tests of QED kernel: (I) Pion-pole contribution to $a_\mu^{\text{HLbL}}$ (cont.)

Result with [VMD model](#) for arbitrary pion mass can easily be obtained from 3-dimensional momentum-space representation (Jegerlehner + AN '09).

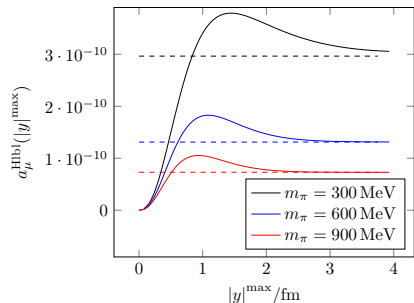
3-dim. integration in position-space:

- $\int_y \rightarrow 2\pi^2 \int_0^\infty d|y| |y|^3$
- $\int_x \rightarrow 4\pi \int_0^\infty d|x| |x|^3 \int_0^\pi d\beta \sin^2 \beta$  (cutoff for  $x$  integration:  $|x|^{\max} = 4.05 \text{ fm}$ )

Integrand after integration over  $|x|, \beta$ :



Result for  $a_\mu^{\text{HLbL}}(|y|^{\max})$ :



- All 6 weight functions contribute to final result, some only at the percent level.
- $|x|^{\max}, |y|^{\max} > 4 \text{ fm}$  needed for  $m_\pi < 300 \text{ MeV}$ .
- For the physical pion mass, one needs to go to very large values of  $|x|$  and  $|y|$ , i.e. very large lattice volumes, to reproduce known result of  $5.7 \cdot 10^{-10}$ .

## Numerical tests of QED kernel: (II) $a_\mu^{\text{LbL}}$ from lepton loop in QED

Fermion propagator in position-space:

$$S_F(x) \equiv \int \frac{d^4 p}{(2\pi)^4} \frac{-ip_\mu \gamma_\mu + m}{p^2 + m^2} e^{ipx} = \frac{m^2}{4\pi^2 |x|} \left[ \gamma_\mu x_\mu \frac{K_2(m|x|)}{|x|} + K_1(m|x|) \right]$$

Analytical result for four-point function in position-space:

$$\begin{aligned} i\widehat{\Pi}_{\rho;\mu\nu\lambda\sigma}(x, y) &= \widehat{\Pi}_{\rho;\mu\nu\lambda\sigma}^{(1)}(x, y) + \widehat{\Pi}_{\rho;\nu\lambda\mu\sigma}^{(1)}(y - x, -x) + \widehat{\Pi}_{\rho;\lambda\nu\mu\sigma}^{(1)}(-x, y - x) \\ &\quad + x_\rho \Pi_{\nu\lambda\mu\sigma}^{(r,1)}(y - x, -x) + x_\rho \Pi_{\lambda\nu\mu\sigma}^{(r,1)}(-x, y - x) \end{aligned}$$

$$\begin{aligned} \Pi_{\mu\nu\lambda\sigma}^{(r,1)}(x, y) &= 2 \left( \frac{m}{2\pi} \right)^8 \left[ \frac{(-x_\alpha)(x-y)_\beta K_2(m|x|)K_2(m|x-y|)}{|x|^2|x-y|^2} \cdot I_{\gamma\delta}(y) \cdot \text{Tr}\{\gamma_\alpha \gamma_\mu \gamma_\beta \gamma_\nu \gamma_\gamma \gamma_\sigma \gamma_\delta \gamma_\lambda\} \right. \\ &\quad + \frac{K_1(m|x|)K_1(m|x-y|)}{|x||x-y|} \cdot p(|y|) \cdot \text{Tr}\{\gamma_\mu \gamma_\nu \gamma_\sigma \gamma_\lambda\} \\ &\quad + \frac{(-x_\alpha)(x-y)_\beta K_2(m|x|)K_2(m|x-y|)}{|x|^2|x-y|^2} \cdot p(|y|) \cdot \text{Tr}\{\gamma_\alpha \gamma_\mu \gamma_\beta \gamma_\nu \gamma_\sigma \gamma_\lambda\} \\ &\quad + \frac{(-x_\alpha) K_2(m|x|)K_1(m|x-y|)}{|x|^2|x-y|} \cdot q_\gamma(y) \cdot \text{Tr}\{\gamma_\alpha \gamma_\mu \gamma_\nu \gamma_\gamma \gamma_\sigma \gamma_\lambda\} \\ &\quad + \frac{(x-y)_\beta K_1(m|x|)K_2(m|x-y|)}{|x||x-y|^2} \cdot q_\gamma(y) \cdot \text{Tr}\{\gamma_\mu \gamma_\beta \gamma_\nu \gamma_\gamma \gamma_\sigma \gamma_\lambda\} \\ &\quad + \frac{(-x_\alpha) K_2(m|x|)K_1(m|x-y|)}{|x|^2|x-y|} \cdot q_\delta(y) \cdot \text{Tr}\{\gamma_\alpha \gamma_\mu \gamma_\nu \gamma_\sigma \gamma_\delta \gamma_\lambda\} \\ &\quad + \frac{(x-y)_\beta K_1(m|x|)K_2(m|x-y|)}{|x||x-y|^2} \cdot q_\delta(y) \cdot \text{Tr}\{\gamma_\mu \gamma_\beta \gamma_\nu \gamma_\sigma \gamma_\delta \gamma_\lambda\} \\ &\quad \left. + \frac{K_1(m|x|)K_1(m|x-y|)}{|x||x-y|} \cdot I_{\gamma\delta}(y) \cdot \text{Tr}\{\gamma_\mu \gamma_\nu \gamma_\gamma \gamma_\sigma \gamma_\delta \gamma_\lambda\} \right] \end{aligned}$$

# The lepton loop (continued)

$$\begin{aligned}
\hat{\Pi}_{\rho;\mu\nu\lambda\sigma}^{(1)}(x, y) = & 2 \left( \frac{m}{2\pi} \right)^8 \left[ \frac{(-x_\alpha)(x-y)_\beta K_2(m|x|)K_2(m|x-y|)}{|x|^2|x-y|^2} \cdot f_{\rho\delta\gamma}(y) \cdot \text{Tr}\{\gamma_\alpha\gamma_\mu\gamma_\beta\gamma_\nu\gamma_\gamma\gamma_\sigma\gamma_\delta\gamma_\lambda\} \right. \\
& + \frac{K_1(m|x|)K_1(m|x-y|)}{|x||x-y|} \cdot f_{\rho\delta\gamma}(y) \cdot \text{Tr}\{\gamma_\mu\gamma_\nu\gamma_\gamma\gamma_\sigma\gamma_\delta\gamma_\lambda\} \\
& + \frac{K_1(m|x|)K_1(m|x-y|)}{|x||x-y|} g_\rho(y) \cdot \text{Tr}\{\gamma_\mu\gamma_\nu\gamma_\sigma\gamma_\lambda\} \\
& + \frac{(-x_\alpha)(x-y)_\beta K_2(m|x|)K_2(m|x-y|)}{|x|^2|x-y|^2} g_\rho(y) \cdot \text{Tr}\{\gamma_\alpha\gamma_\mu\gamma_\beta\gamma_\nu\gamma_\sigma\gamma_\lambda\} \\
& + \frac{(-x_\alpha) K_2(m|x|)K_1(m|x-y|)}{|x|^2|x-y|} h_{\rho\gamma}(y) \cdot \text{Tr}\{\gamma_\alpha\gamma_\mu\gamma_\nu\gamma_\gamma\gamma_\sigma\gamma_\lambda\} \\
& + \frac{(x-y)_\beta K_1(m|x|)K_2(m|x-y|)}{|x||x-y|^2} h_{\rho\gamma}(y) \cdot \text{Tr}\{\gamma_\mu\gamma_\beta\gamma_\nu\gamma_\gamma\gamma_\sigma\gamma_\lambda\} \\
& + \frac{(-x_\alpha) K_2(m|x|)K_1(m|x-y|)}{|x|^2|x-y|} \hat{f}_{\rho\delta}(y) \cdot \text{Tr}\{\gamma_\alpha\gamma_\mu\gamma_\nu\gamma_\sigma\gamma_\delta\gamma_\lambda\} \\
& \left. + \frac{(x-y)_\beta K_1(m|x|)K_2(m|x-y|)}{|x||x-y|^2} \hat{f}_{\rho\delta}(y) \cdot \text{Tr}\{\gamma_\mu\gamma_\beta\gamma_\nu\gamma_\sigma\gamma_\delta\gamma_\lambda\} \right]
\end{aligned}$$

$$I_{\gamma\delta}(y) = \frac{2\pi^2}{m^2} \left( \hat{y}_\gamma \hat{y}_\delta K_2(m|y|) - \delta_{\gamma\delta} \frac{K_1(m|y|)}{m|y|} \right), \quad h_{\rho\gamma}(y) = \frac{\pi^2}{m^3} \left( \hat{y}_\gamma \hat{y}_\rho m|y| K_1(m|y|) - \delta_{\gamma\rho} K_0(m|y|) \right),$$

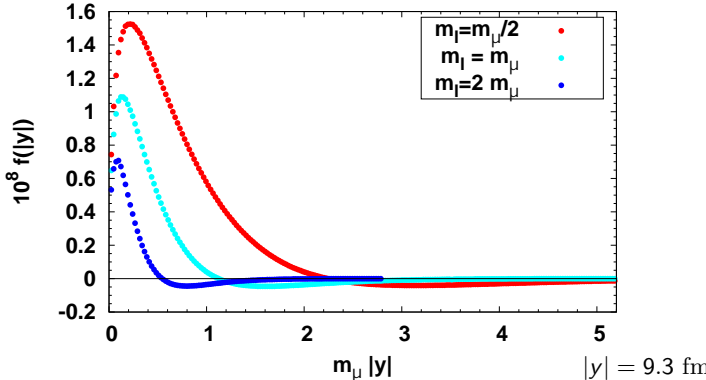
$$\hat{f}_{\rho\delta}(y) = \frac{\pi^2}{m^3} \left\{ \hat{y}_\rho \hat{y}_\delta m|y| K_1(m|y|) + \delta_{\rho\delta} K_0(m|y|) \right\}, \quad q_\gamma(y) = \frac{2\pi^2}{m^2} \hat{y}_\gamma K_1(m|y|),$$

$$f_{\rho\delta\gamma}(y) = \frac{\pi^2}{m^3} \left\{ \hat{y}_\gamma \hat{y}_\delta \hat{y}_\rho m|y| K_2(m|y|) + (\delta_{\rho\delta} \hat{y}_\gamma - \delta_{\gamma\rho} \hat{y}_\delta - \delta_{\gamma\delta} \hat{y}_\rho) K_1(m|y|) \right\}, \quad \rho(|y|) = \frac{2\pi^2}{m^2} K_0(m|y|)$$

$$\hat{y} = y/|y|$$

## Lepton loop contribution $a_{\mu}^{\text{LbL}}$ in QED

Integrand of lepton loop contribution  $a_{\mu}^{\text{LbL}}$ :



$m_l/m_\mu$	$a_{\mu}^{\text{LbL}} \times 10^{11}$ (exact)	$a_{\mu}^{\text{LbL}} \times 10^{11}$	Precision	Deviation
1/2	1229.07	1257.5(6.2)(2.4)	0.5%	2.3%
1	464.97	470.6(2.3)(2.1)	0.7%	1.2%
2	150.31	150.4(0.7)(1.7)	1.2%	0.06%

1st uncertainty from 3D integration, 2nd uncertainty from extrapolation to small  $|y|$ .

Behavior for small  $|y|$  compatible with  $f(|y|) \propto m_\mu |y| \log^2(m_\mu |y|)$ .

Analytical results for  $a_{\mu}^{\text{LbL}}$  with  $m_l = m_\mu, 2m_\mu$  reproduced at the percent level.

(Laporta + Remiddi '93, numbers courtesy of Massimo Passera)

Part II: Lattice calculation of the pion transition  
form factor  $\pi^0 \rightarrow \gamma^* \gamma^*$

# $\mathcal{F}_{\pi^0\gamma^*\gamma^*}(q_1^2, q_2^2)$ from lattice QCD

Gérardin, Meyer, AN, PRD 94, 074507 (2016)

Pion-pole (pseudoscalar-pole) contribution to HLBL numerically dominant.

Earlier exploratory studies of form factor at rather large pion mass and single lattice spacing by Dudek + Edwards '06; Cohen *et al.* '08; Lin + Cohen '12; Shintani *et al.* '09; Feng *et al.* '11 or interested more in low-energy region ( $\pi^0 \rightarrow \gamma\gamma$ ), Feng *et al.* '12.

Lattice setup for our analysis (CLS ensembles):

- $N_f = 2$  dynamical quarks
- Pion masses in the range [190 – 440] MeV
- 3 lattice spacings:  $a = (0.048, 0.065, 0.075)$  fm
- Photon virtualities up to  $Q_{1,2}^2 \sim 1.5$  GeV $^2$

In Euclidean space-time: [Cohen *et al.* '08; Feng *et al.* '12]

$$\begin{aligned} M_{\mu\nu}^E(p, q_1) &= - \int d\tau e^{\omega_1 \tau} \int d^3z e^{-i\vec{q}_1 \vec{z}} \langle 0 | T \left\{ J_\mu(\vec{z}, \tau) J_\nu(\vec{0}, 0) \right\} | \pi(p) \rangle \\ &= \epsilon_{\mu\nu\alpha\beta} q_{1\alpha} q_{2\beta} \mathcal{F}_{\pi^0\gamma^*\gamma^*}(q_1^2, q_2^2) \end{aligned}$$

- Analytical continuation
- We must keep  $q_{1,2}^2 < M_V^2 = \min(M_\rho^2, 4m_\pi^2)$  to avoid poles
- $q_1 = (\omega_1, \vec{q}_1)$

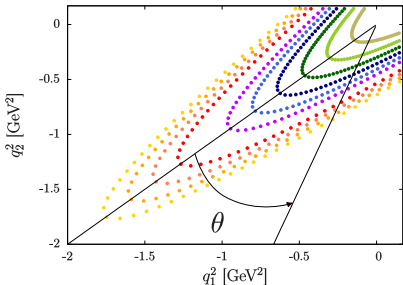
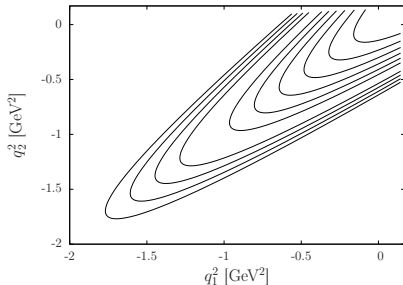
Actually, the main object to compute is the three-point correlation function:

$$C_{\mu\nu}^{(3)}(\tau, t_\pi; \vec{p}, \vec{q}_1, \vec{q}_2) = \sum_{\vec{x}, \vec{z}} \langle T \left\{ J_\nu(\vec{0}, t_f) J_\mu(\vec{z}, t_i) P(\vec{x}, t_0) \right\} \rangle e^{i\vec{p}\vec{x}} e^{-i\vec{q}_1 \vec{z}}$$

## Kinematic reach in the photon virtualities

We choose  $\vec{p} = \vec{0}$  (pion at rest)  $\Rightarrow \begin{cases} q_1^2 = \omega_1^2 - |\vec{q}_1|^2 \\ q_2^2 = (m_\pi - \omega_1)^2 - |\vec{q}_1|^2 \end{cases}$

- Momenta on lattice are discrete :  $|\vec{q}_1|^2 = \left(\frac{2\pi}{L}\right)^2 |\vec{n}|^2$  ,  $|\vec{n}|^2 = 1, 2, 3, 4, 5, \dots$
- $\omega_1$  is a free parameter:  $q_1 = (\omega_1, \vec{q}_1)$
- By varying continuously  $\omega_1$  we have access to different values of  $(q_1^2, q_2^2)$
- Access only to certain subsets of mostly spacelike photon momenta in  $(q_1^2, q_2^2)$ -plane
- In practice: sample discrete values of  $\omega_1$
- $\tan(\theta - \pi/4) = q_1^2/q_2^2$
- Example:  $64^3 \times 128$  lattice at  $a = 0.048$  fm,  $m_\pi = 268$  MeV



## Comparison of lattice data with phenomenological models

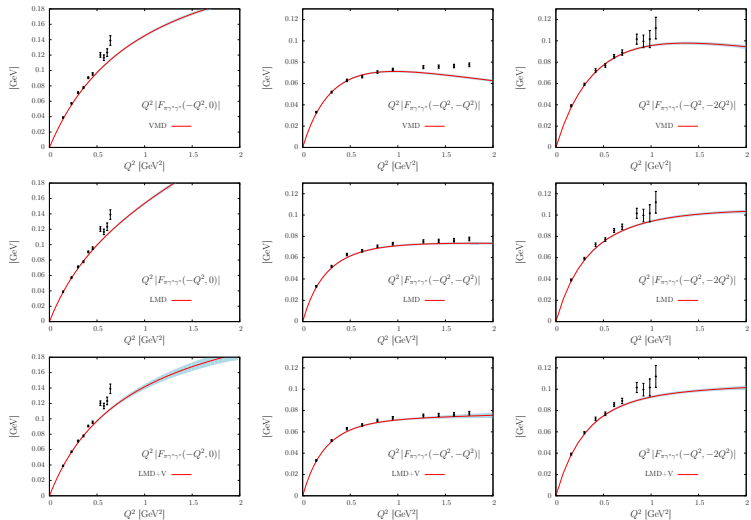
- Models: VMD, LMD, LMD+V
- Local fit: each ensemble is fitted independently, then chiral and continuum extrapolation for model parameters.
- Global fit: combined chiral and continuum extrapolation for all model parameters.
- LMD+V: too many model parameters, only global fit is stable (with additional assumptions on some model parameters).
- **VMD model fails to describe data:  $\chi^2/\text{d.o.f.} = 2.9$  (uncorrelated global fit).**

In particular double-virtual form factor at large momenta. Also do not recover anomaly (normalization at origin) and  $\rho$ -mass for  $M_V^{\text{VMD}}$ .

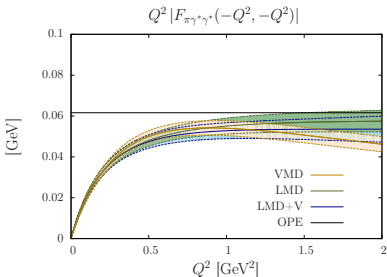
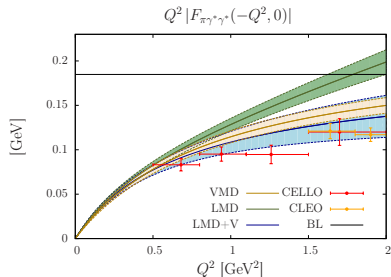
- **Data well described by LMD model:  $\chi^2/\text{d.o.f.} = 1.3$  (uncorrelated global fit).**  
Might be surprising as the LMD form factor  $\mathcal{F}_{\pi^0 \gamma^* \gamma^*}^{\text{LMD}}(-Q^2, 0)$  has the wrong asymptotic behavior, but largest  $Q^2$  only  $\simeq 1.5 \text{ GeV}^2$  on lattice. Reproduce anomaly to 7% accuracy and even prediction for OPE.
- **Data well described by LMD+V model:  $\chi^2/\text{d.o.f.} = 1.4$  (uncorrelated global fit).**  
Reproduce anomaly to 9% accuracy and with quite large uncertainty, phenomenological estimates of model parameters  $\bar{h}_2 = -10.63 \text{ GeV}^2$  and  $h_5 = (6.93 \pm 0.26) \text{ GeV}^4$  (Knecht + AN '01; Melnikov + Vainshtein '04).

# Comparison of lattice data with phenomenological models (continued)

Ensemble O7 (compared to result of global fit)  
 $[a = 0.048 \text{ fm}, m_\pi = 268 \text{ MeV}]$



# Final results for $\pi^0$ transition form factor at the physical point



**LMD model** ( $\chi^2/\text{d.o.f.} = 1.3$ , uncorrelated global fit)

$$\alpha^{\text{LMD}} = 0.275(18)(3) \text{ GeV}^{-1}, \beta = -0.028(4)(1) \text{ GeV}, M_V^{\text{LMD}} = 0.705(24)(21) \text{ GeV}$$

$$(\alpha^{\text{th}} = 1/(4\pi^2 F_\pi)) = 0.274 \text{ GeV}^{-1}, \beta^{\text{OPE}} = -F_\pi/3 = -0.0308 \text{ GeV}$$

**LMD+V model** ( $\chi^2/\text{d.o.f.} = 1.4$ , uncorrelated global fit)

$$\alpha^{\text{LMD+V}} = 0.273(24)(7) \text{ GeV}^{-1}, \bar{h}_2 = -11.2(5.4)(2.7) \text{ GeV}^2, \bar{h}_5 = 8.5(2.9)(1.4) \text{ GeV}^4$$

$$(\tilde{h}_0 = -F_\pi/3 = -0.0308 \text{ GeV}, \tilde{h}_1 = 0, M_{V_1} = 0.775 \text{ GeV}, M_{V_2} = 1.465 \text{ GeV fixed at physical point})$$

Systematic errors:

- Finite-time extent of the lattice
- Finite-size effects (no dedicated study, data suggest rather small effect)
- Disconnected contributions: below 1% for 1 ensemble ( $m_\pi = 440$  MeV).

# Pion-pole contribution to $a_\mu^{\text{HLbL};\pi^0}$ from lattice QCD

Using the LMD+V model from our global fit to the lattice data, we obtain as our preferred estimate:

$$a_{\mu;\text{LMD+V}}^{\text{HLbL};\pi^0} = (65.0 \pm 8.3) \times 10^{-11} \quad (\pm 12.8\%)$$

Error from covariance matrix is statistical only.

Model	$a_\mu^{\text{HLbL};\pi^0} \times 10^{11}$
LMD (lattice fit)	68.2(7.4)
LMD+V (lattice fit)	65.0(8.3)
VMD (theory)	57.0
LMD (theory)	73.7
LMD+V (theory + pheno)	62.9

Most model calculations yield results in the range  $a_\mu^{\text{HLbL};\pi^0} = (50 - 80) \times 10^{-11}$ .

$a_\mu^{\text{HLbL};\pi^0}$  in units of  $10^{-11}$ , integrated up to some momentum cutoff  $\Lambda$ :

$\Lambda$ [GeV]	LMD	LMD+V
0.25	14.6 (21.4%)	14.4 (22.1%)
0.5	37.9 (55.5%)	37.2 (57.2%)
0.75	50.7 (74.4%)	49.5 (76.1%)
1.0	57.3 (84.0%)	55.5 (85.4%)
1.5	62.9 (92.3%)	60.6 (93.1%)
2.0	65.1 (95.5%)	62.5 (96.1%)
5.0	67.7 (99.2%)	64.6 (99.4%)
20.0	68.2 (100%)	65.0 (100%)

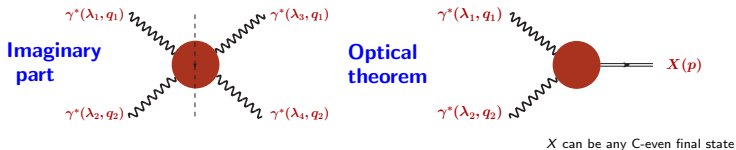
Even though the LMD and LMD+V models give almost equally good fits to the lattice data, they differ for large momenta, in particular for the single-virtual form factor. LMD does not obey Brodsky-Lepage behavior.

## Part III: Light-by-light forward scattering amplitudes in lattice QCD

# Forward HLbL scattering amplitudes and dispersion relations

Gérardin et al., Lattice 2017 and work in preparation.

## Optical theorem

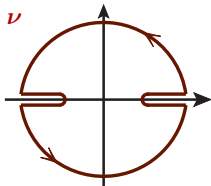


$$W_{\lambda_3 \lambda_4, \lambda_1 \lambda_2} = \text{Abs } M_{\lambda_3 \lambda_4, \lambda_1 \lambda_2} = \frac{1}{2} \int d\Gamma_X (2\pi)^4 \delta(q_1 + q_2 - p_X) \mathcal{M}_{\lambda_1 \lambda_2}(q_1, q_2, p_X) \mathcal{M}_{\lambda_3 \lambda_4}^*(q_1, q_2, p_X)$$

81 helicity amplitudes  $M_{\lambda'_1 \lambda'_2, \lambda_1 \lambda_2}$  ( $\lambda_i^{(i)} = 0, \pm 1$ , off-shell photons) reduce to 8 independent forward scattering amplitudes (parity and time invariance).

## Dispersion relations [Pascalutsa et al. '12]

Once-subtracted dispersion relation: crossing-symmetric variable  $\nu = q_1 \cdot q_2$



$$M_{\text{even}}(\nu) = M_{\text{even}}(0) + \frac{2\nu^2}{\pi} \int_{\nu_0}^{\infty} d\nu' \frac{1}{\nu'(\nu'^2 - \nu^2 - i\epsilon)} W_{\text{even}}(\nu')$$

$$M_{\text{odd}}(\nu) = \nu M_{\text{odd}}(0) + \frac{2\nu^3}{\pi} \int_{\nu_0}^{\infty} d\nu' \frac{1}{\nu'(\nu'^2 - \nu^2 - i\epsilon)} W_{\text{odd}}(\nu')$$

Higher mass singularities are suppressed with  $\nu^2 \Rightarrow$  only a few states  $X$  necessary to saturate dispersion relation and reproduce lattice data.

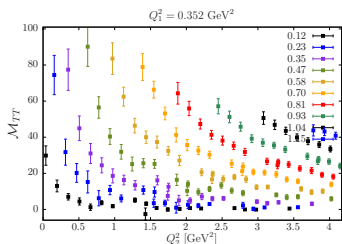
# Description of the lattice data using phenomenology

For each of the eight amplitudes, we have a dispersion relation:

$$\overline{M}_\alpha(\nu) = \frac{4\nu^2}{\pi} \int_{\nu_0}^{\infty} d\nu' \frac{\sqrt{X'} \sigma_\alpha / \tau_\alpha(\nu')}{\nu'(\nu'^2 - \nu^2 - i\epsilon)}$$

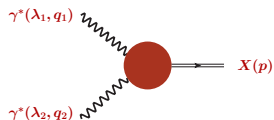
## Left-hand side: Lattice calculation

From 4-point correlation function get amplitudes for different values of  $Q_1^2, Q_2^2, \nu = q_1 \cdot q_2$  (different colors).



## Right-hand side: fusion cross sections

$$\gamma^*(\lambda_1, q_1) + \gamma^*(\lambda_2, q_2) \rightarrow X(p_X)$$



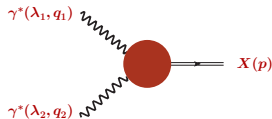
X: any C-even state contributes.

Main contribution is expected from mesons:

Pseudoscalars ( $0^{-+}$ )   Axial-vectors ( $1^{++}$ )  
Scalar ( $0^{++}$ )              Tensors ( $2^{++}$ )

Consider only one particle in each channel.

## Two-photon fusion cross sections: modelling



- Example: contribution of the pseudoscalar to the amplitude  $M_{TT}$ :

$$\sigma_{TT} = 8\pi^2 \delta(s - m_P^2) \frac{2\sqrt{X}}{m_P^2} \times \frac{\Gamma_{\gamma\gamma}}{m_P} \times \left[ \frac{F_{P\gamma^*\gamma^*}(Q_1^2, Q_2^2)}{F_{P\gamma^*\gamma^*}(0, 0)} \right]^2$$

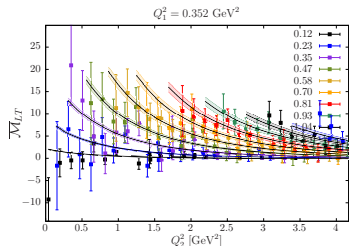
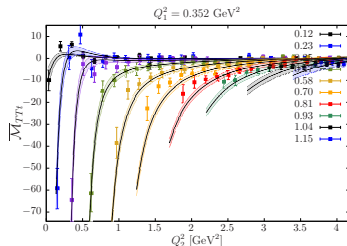
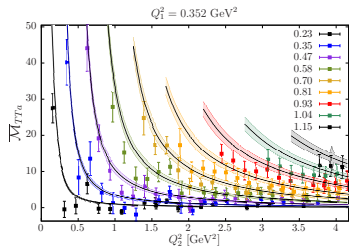
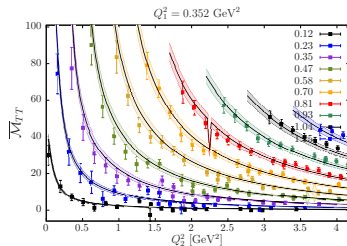
- Similar results for other mesons (assume Breit-Wigner shape for resonances).
- In general, the two-photon decay width is taken from experiment, e.g. for the scalars  $\Gamma_{\gamma\gamma} = \frac{\pi\alpha^2}{4} ms \left[ F_{S\gamma^*\gamma^*}^T(0, 0) \right]^2$ , except for the pseudoscalars, where lattice data is used [Gérardin et al. '16].
- All the non-perturbative information is encoded in the meson transition form factors  $F_{X\gamma^*\gamma^*}(Q_1^2, Q_2^2)$ .
- Assume monopole or dipole ansatz for transition form factors (parametrized by one mass scale  $\Lambda_X$ ):

$$F_X(Q_1^2, Q_2^2) = \frac{F_X(0, 0)}{(1 + Q_1^2/\Lambda_X^2)(1 + Q_2^2/\Lambda_X^2)}$$

$$F_X(Q_1^2, Q_2^2) = \frac{F_X(0, 0)}{(1 + Q_1^2/\Lambda_X^2)^2(1 + Q_2^2/\Lambda_X^2)^2}$$

## Preliminary results: Ensemble F6 - dependence on $\nu$ and $Q_2^2$

- $m_\pi = 314$  MeV, lattice spacing  $a = 0.065$  fm.
- Each plot correspond to a fixed  $Q_1^2 = 0.352$  GeV $^2$ .
- Different colors correspond to different values of  $\nu = q_1 \cdot q_2$ .
- Get a good description of the lattice data for most ensembles with  $\chi^2/\text{d.o.f.} \sim 1.13 - 1.35$  (E5 with  $m_\pi = 437$  MeV not well described).



# Conclusions

## Part I

- Explicit master formula for  $a_\mu^{\text{HLbL}}$  in position-space.
- QED kernel function (in continuum and infinite volume to avoid power-law effects  $1/L^2$ ) multiplying the position-space four-point correlation function.  
→ 6 weight functions stored on disk, ready to be used.
- Verified QED kernel function by evaluating pion-pole contribution in VMD model and lepton-loop in QED (agreement with known results).
- Need rather large lattices  $L > 5 \text{ fm}$  to reproduce results for  $m_\pi < 300 \text{ MeV}$  and for  $m_{\text{loop}} \leq m_\mu$ .

## Part II

- Performed calculation of pion transition form factor  $\mathcal{F}_{\pi^0\gamma^*\gamma^*}(-Q_1^2, -Q_2^2)$  on lattice with 2 dynamical quarks for spacelike momenta  $Q_i^2 \leq 1.5 \text{ GeV}^2$ .
- VMD model fails to describe lattice data, especially in double-virtual case.
- LMD and LMD+V models describe our data successfully.
- First lattice calculation of pion-pole contribution (only statistical error):

$$a_{\mu; \text{LMD+V}}^{\text{HLbL}; \pi^0} = (65.0 \pm 8.3) \times 10^{-11}$$

## Part III

- Eight forward HLbL scattering amplitudes computed on lattice.
- Well described by the cross sections  $\gamma^*\gamma^* \rightarrow \text{a few resonances}$  via dispersion relations.
- Allows to constrain transition form factors used to estimate  $a_\mu^{\text{HLbL}}$ .

## Backup slides

## Vertex function for HLbL in momentum space

In Euclidean space ( $k = p' - p$ ):

$$\langle \mu^-(p', s') | j_\rho(0) | \mu^-(p, s) \rangle = -\bar{u}^{s'}(p') \left[ \gamma_\rho F_1(k^2) + \frac{\sigma_{\rho\tau} k_\tau}{2m} F_2(k^2) \right] u^s(p)$$

Project on anomalous magnetic moment:

$$a_\mu^{\text{HLbL}} = F_2(0) = \frac{-i}{48m} \text{Tr}\{[\gamma_\rho, \gamma_\sigma](-i\cancel{p} + m)\Gamma_{\rho\sigma}(p, p)(-i\cancel{p} + m)\}$$

with on-shell muon momentum  $p = im\hat{\epsilon}$  ( $p^2 = -m^2$ ;  $\hat{\epsilon}$ : unit vector).

$$\begin{aligned} \Gamma_{\rho\sigma}(p', p) &= -e^6 \int_{q_1, q_2} \frac{1}{q_1^2 q_2^2 (q_1 + q_2 - k)^2} \frac{1}{(p' - q_1)^2 + m^2} \frac{1}{(p' - q_1 - q_2)^2 + m^2} \\ &\quad \times \gamma_\mu(i\cancel{p}' - i\cancel{q}_1 - m) \gamma_\nu(i\cancel{p} - i\cancel{q}_1 - i\cancel{q}_2 - m) \gamma_\lambda \\ &\quad \times \frac{\partial}{\partial k_\rho} \Pi_{\mu\nu\lambda\sigma}(q_1, q_2, k - q_1 - q_2) \end{aligned}$$

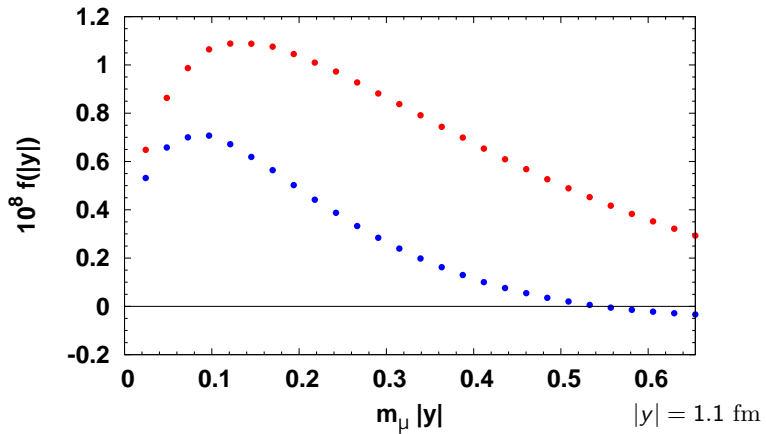
$$\Pi_{\mu\nu\lambda\sigma}(q_1, q_2, q_3) = \int_{x_1, x_2, x_3} e^{-i(q_1 x_1 + q_2 x_2 + q_3 x_3)} \langle j_\mu(x_1) j_\nu(x_2) j_\lambda(x_3) j_\sigma(0) \rangle$$

Where we used the following relation derived from the Ward identities to extract one factor of  $k$  to get  $F_2(k^2)$  [Kinoshita et al. '70]:

$$\Pi_{\mu\nu\lambda\rho}(q_1, q_2, k - q_1 - q_2) = -k_\sigma \frac{\partial}{\partial k_\rho} \Pi_{\mu\nu\lambda\sigma}(q_1, q_2, k - q_1 - q_2)$$

Notation:  $\int_q \equiv \int \frac{d^4 q}{(2\pi)^4}$ ,  $\int_x \equiv \int d^4 x$

## Integrand of lepton loop contribution $a_\mu^{\text{LbL}}$ (zoom)

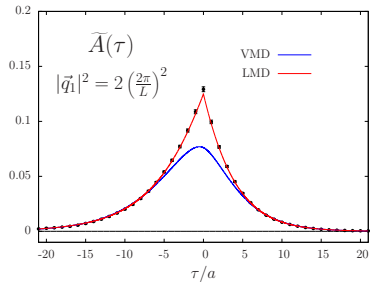


Behavior for small  $|y|$  numerically compatible with  $f(|y|) \propto m_\mu |y| \log^2(m_\mu |y|)$ .

## Shape of integrand for ensemble F7

( $a = 0.065$  fm and  $m_\pi = 270$  MeV)

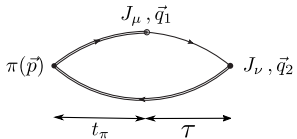
$$M_{\mu\nu}^E = \frac{2E_\pi}{Z_\pi} \int_{-\infty}^{\infty} d\tau \tilde{A}_{\mu\nu}(\tau) e^{\omega_1 \tau} e^{-E_\pi \tau}$$



Cusp at  $\tau = 0$  related to OPE  
(coefficient  $\beta \neq 0$  in LMD model)

$$A_{\mu\nu}(\tau) = \lim_{t_\pi \rightarrow \infty} C_{\mu\nu}(\tau, t_\pi) e^{E_\pi t_\pi}$$

$$\tilde{A}_{\mu\nu}(\tau) = \begin{cases} A_{\mu\nu}(\tau) & \tau > 0 \\ A_{\mu\nu}(\tau) e^{-E_\pi \tau} & \tau < 0 \end{cases}$$



Finite time extent of the lattice:

→ Fit the data at large  $\tau$  using a vector meson dominance (VMD) model or lowest meson dominance (LMD) model:

$$\mathcal{F}_{\pi^0 \gamma^* \gamma^*}^{\text{VMD}}(q_1^2, q_2^2) = \frac{\alpha M_V^4}{(M_V^2 - q_1^2)(M_V^2 - q_2^2)}$$

$$\mathcal{F}_{\pi^0 \gamma^* \gamma^*}^{\text{LMD}}(q_1^2, q_2^2) = \frac{\alpha M_V^4 + \beta(q_1^2 + q_2^2)}{(M_V^2 - q_1^2)(M_V^2 - q_2^2)}$$

→ Introduces a cut-off  $\tau_c \gtrsim 1.3$  fm

# Slope of $\pi^0$ form factor from lattice QCD

Reminder:

$$b_{\pi^0} = \frac{1}{\mathcal{F}_{\pi^0\gamma^*\gamma^*}(0,0)} \left. \frac{d\mathcal{F}_{\pi^0\gamma^*\gamma^*}(q^2, 0)}{dq^2} \right|_{q^2=0}$$

Recent theoretical estimates:

$$\begin{aligned} b_{\pi^0}^{\text{Pad\'e}} &= (1.78 \pm 0.12) \text{ GeV}^{-2} \quad (\pm 6.9\%) \quad (\text{Masjuan '12}) \\ b_{\pi^0}^{\text{DR}} &= (1.69 \pm 0.03) \text{ GeV}^{-2} \quad (\pm 2\%) \quad (\text{Hoferichter et al. '14}) \end{aligned}$$

Fits to lattice data:

$$\begin{aligned} b_{\pi^0}^{\text{LMD,fit}} &= (1.60 \pm 0.11) \text{ GeV}^{-2} \quad (\pm 6.8\%) \\ b_{\pi^0}^{\text{LMD+V,fit}} &= (1.58 \pm 0.23) \text{ GeV}^{-2} \quad (\pm 14.3\%) \end{aligned}$$

Errors from covariance matrix are statistical only. Results well compatible with each other. Do not consider VMD model (bad fit of lattice data, wrong normalization at origin,  $M_V^{\text{VMD}}$  differs from expected  $m_\rho$ ).

Experimental determinations:

$$\begin{aligned} b_{\pi^0}^{\text{PDG}} &= (1.76 \pm 0.22) \text{ GeV}^{-2} \quad (\pm 12.5\%) \\ b_{\pi^0}^{\text{NA62}} &= (2.03 \pm 0.35) \text{ GeV}^{-2} \quad (\pm 17.2\%) \\ b_{\pi^0}^{\text{A2}} &= (1.65 \pm 0.55) \text{ GeV}^{-2} \quad (\pm 33\%) \end{aligned}$$

PDG value essentially from spacelike CELLO data (VMD fit, extrapolated from  $Q^2 \geq 0.5 \text{ GeV}^2$  to origin). Confirmed within uncertainties by recent timelike measurements at low  $|q|$  by NA48/2 + NA62 and A2.

## Comparison of lattice data with phenomenological models (1): VMD

$$\mathcal{F}_{\pi^0 \gamma^* \gamma^*}^{\text{VMD}}(q_1^2, q_2^2) = \frac{\alpha M_V^4}{(M_V^2 - q_1^2)(M_V^2 - q_2^2)}$$

	$\mathcal{F}_{\pi^0 \gamma^* \gamma^*}(0, 0)$	$\mathcal{F}_{\pi^0 \gamma^* \gamma^*(-Q^2, 0)}$	$\mathcal{F}_{\pi^0 \gamma^* \gamma^*(-Q^2, -Q^2)}$
VMD	$\alpha$	$\alpha M_V^2 / Q^2$	$\alpha M_V^4 / Q^4$
Theory	$1/(4\pi^2 F_\pi)$	$2F_\pi / Q^2$	$2F_\pi / (3Q^2)$

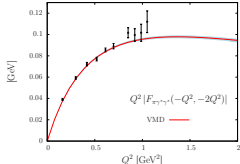
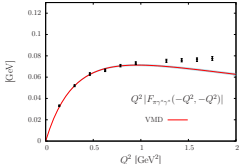
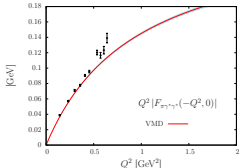
## Two fitting procedures:

- Local fit: each ensemble is fitted independently ( $\alpha(a, m_\pi^2)$ ,  $M_V(a, m_\pi^2)$ ) + chiral and continuum extrapolation
  - Global fit: combined chiral and continuum extrapolation → 6 fit param.

$$\alpha^{\text{VMD}} = 0.243(18) \text{ GeV}^{-1}, \quad M_V^{\text{VMD}} = 0.944(34) \text{ GeV}$$

$\chi^2/\text{d.o.f.} = 2.9$  (uncorrelated global fit). VMD model fails to describe our data.

In particular double-virtual form factor at large momenta. Also do not recover anomaly  $\alpha^{\text{VMD}} \neq \alpha^{\text{th}} = 1/(4\pi^2 F_\pi) = 0.274 \text{ GeV}^{-1}$  and  $\rho$ -mass for  $M_V^{\text{VMD}}$ .



## Comparison (2): LMD (Lowest meson dominance)

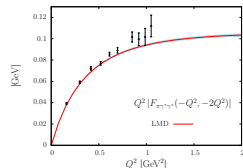
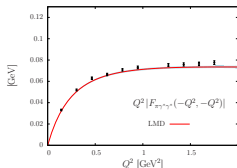
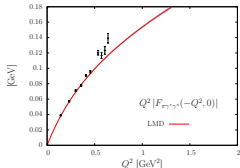
$$\mathcal{F}_{\pi^0 \gamma^* \gamma^*}^{\text{LMD}}(q_1^2, q_2^2) = \frac{\alpha M_V^4 + \beta(q_1^2 + q_2^2)}{(M_V^2 - q_1^2)(M_V^2 - q_2^2)}$$

Large- $N_c$  approximation to QCD  
[Moussallam '95; Knecht *et al.* '99]

	$\mathcal{F}_{\pi^0 \gamma^* \gamma^*}(0, 0)$	$\mathcal{F}_{\pi^0 \gamma^* \gamma^*}(-Q^2, 0)$	$\mathcal{F}_{\pi^0 \gamma^* \gamma^*}(-Q^2, -Q^2)$
LMD	$\alpha$	$-\beta/M_V^2$	$-2\beta/Q^2$
Theory	$1/(4\pi^2 F_\pi)$	$2F_\pi/Q^2$	$2F_\pi/(3Q^2)$
	✓	(Brodsky-Lepage) X	(OPE) ✓

$$\alpha^{\text{LMD}} = 0.275(18) \text{ GeV}^{-1}, \quad \beta = -0.028(4) \text{ GeV}, \quad M_V^{\text{LMD}} = 0.705(24) \text{ GeV}$$

- $\chi^2/\text{d.o.f.} = 1.3$  (uncorrelated global fit). Data well described by LMD model.
- Might be surprising as the form factor  $\mathcal{F}_{\pi^0 \gamma^* \gamma^*}^{\text{LMD}}(-Q^2, 0)$  has the wrong asymptotic behavior, but largest  $Q^2$  only  $\simeq 1.5 \text{ GeV}^2$  on lattice.
- $\alpha^{\text{LMD}}$  is compatible with theoretical prediction  $\alpha^{\text{th}} = 1/(4\pi^2 F_\pi) = 0.274 \text{ GeV}^{-1} \rightarrow$  accuracy 7%
- $\beta$  is compatible with OPE prediction  $\beta^{\text{OPE}} = -F_\pi/3 = -0.0308 \text{ GeV}$



## Comparison (3): LMD+V

$$\mathcal{F}_{\pi^0 \gamma^* \gamma^*}^{LMD+V}(q_1^2, q_2^2) = \frac{\tilde{h}_0 q_1^2 q_2^2 (q_1^2 + q_2^2) + \tilde{h}_1 (q_1^2 + q_2^2)^2 + \tilde{h}_2 q_1^2 q_2^2 + \tilde{h}_5 M_{V_1}^2 M_{V_2}^2 (q_1^2 + q_2^2) + \alpha M_{V_1}^4 M_{V_2}^4}{(M_{V_1}^2 - q_1^2)(M_{V_2}^2 - q_1^2)(M_{V_1}^2 - q_2^2)(M_{V_2}^2 - q_2^2)}$$

	$\mathcal{F}_{\pi^0 \gamma^* \gamma^*}(0, 0)$	$\mathcal{F}_{\pi^0 \gamma^* \gamma^*}(-Q^2, 0)$	$\mathcal{F}_{\pi^0 \gamma^* \gamma^*}(-Q^2, -Q^2)$
LMD+V	$\alpha$	$-\tilde{h}_5/Q^2$	$-2\tilde{h}_0/Q^2$
Theory	$1/(4\pi^2 F_\pi)$	$2F_\pi/Q^2$ (Brodsky-Lepage) ✓	$2F_\pi/(3Q^2)$ (OPE) ✓

- Refinement of the LMD model which satisfies OPE and Brodsky-Lepage → include a second vector resonance,  $\rho'$  [Knecht + AN '01].
- All the theoretical constraints are satisfied if one sets  $\tilde{h}_1 = 0$ .
- But the number of parameters also increases (local fits are unstable, global fit only).
- Assumptions in global fit:
  - $\tilde{h}_1 = 0$
  - $\tilde{h}_0 = \tilde{h}_0^{\text{OPE}} = -F_\pi/3$
  - $M_{V_1} = m_\rho^{\text{exp}} = 0.775$  GeV in the continuum and at physical pion mass (but chiral corrections are taken into account in the fit).
  - Constant shift in the spectrum:  $M_{V_2}(\tilde{y}) = m_{\rho'}^{\text{exp}} + M_{V_1}(\tilde{y}) - m_\rho^{\text{exp}}$  with  $m_{\rho'}^{\text{exp}} = 1.465$  GeV and  $\tilde{y} = m_\pi^2/(8\pi^2 F_\pi^2)$ .

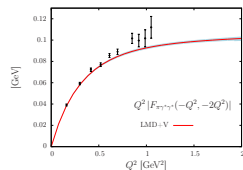
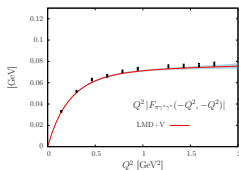
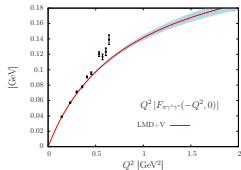
## Comparison (3): LMD+V (continued)

$$\mathcal{F}_{\pi^0 \gamma^* \gamma^*}^{LMD+V}(q_1^2, q_2^2) = \frac{\tilde{h}_0 q_1^2 q_2^2 (q_1^2 + q_2^2) + \tilde{h}_1 (q_1^2 + q_2^2)^2 + \tilde{h}_2 q_1^2 q_2^2 + \tilde{h}_5 M_{V1}^2 M_{V2}^2 (q_1^2 + q_2^2) + \alpha M_{V1}^4 M_{V2}^4}{(M_{V1}^2 - q_1^2)(M_{V2}^2 - q_1^2)(M_{V1}^2 - q_2^2)(M_{V2}^2 - q_2^2)}$$

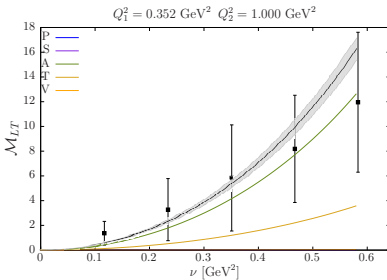
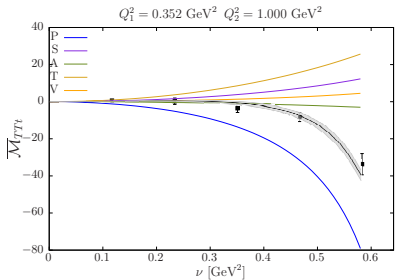
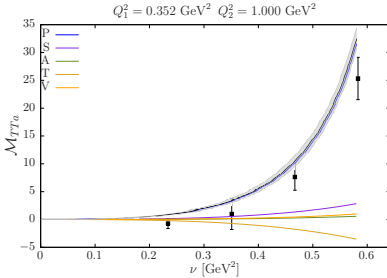
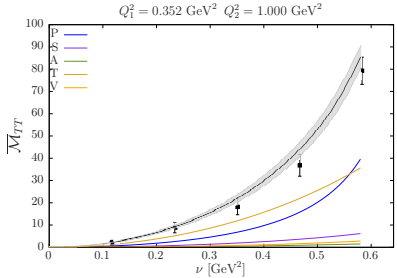
	$\mathcal{F}_{\pi^0 \gamma^* \gamma^*}(0, 0)$	$\mathcal{F}_{\pi^0 \gamma^* \gamma^*}(-Q^2, 0)$	$\mathcal{F}_{\pi^0 \gamma^* \gamma^*}(-Q^2, -Q^2)$
LMD+V	$\alpha$	$-\tilde{h}_5/Q^2$	$-2\tilde{h}_0/Q^2$
Theory	$1/(4\pi^2 F_\pi)$	$2F_\pi/Q^2$	$2F_\pi/(3Q^2)$
	✓	(Brodsky-Lepage) ✓	(OPE) ✓

$$\alpha^{LMD+V} = 0.273(24) \text{ GeV}^{-1}, \quad \tilde{h}_2 = 0.345(167) \text{ GeV}^3, \quad \tilde{h}_5 = -0.195(70) \text{ GeV}$$

- $\chi^2/\text{d.o.f.} = 1.4$  (uncorrelated global fit). Data well described by LMD+V model.
- $\alpha^{LMD+V}$  is again compatible with the theoretical prediction  
 $\alpha^{\text{th}} = 1/(4\pi^2 F_\pi) = 0.274 \text{ GeV}^{-1} \rightarrow$  accuracy 9%
- $\tilde{h}_2$  and  $\tilde{h}_5$  agree with phenomenological estimates [Knecht + AN '01; Melnikov + Vainshtein '04].



# Preliminary results: F6 - contributions from different channels



V = scalar QED dressed with monopole form factors (mass set to lattice rho mass).

## Preliminary results: monopole and dipole masses

- Global fit of the eight forward scattering amplitudes [Preliminary results]

	$M_S$ [GeV]	$M_A$ [GeV]	$M_T^{(2)}$ [GeV]	$M_T^{(0,T)}$ [GeV]	$M_T^{(1)}$ [GeV]	$M_T^{(0,L)}$ [GeV]	$\chi^2/\text{d.o.f.}$
E5	1.38(11)	1.26(10)	1.93(3)	2.24(5)	2.36(4)	0.60(10)	4.22(59)
F6	1.12(14)	1.44(5)	1.66(9)	2.17(5)	1.85(14)	0.89(28)	1.15(20)
F7	1.04(18)	1.29(8)	1.61(12)	2.08(7)	2.03(7)	0.57(16)	1.19(18)
G8	1.07(10)	1.36(5)	1.37(24)	2.03(6)	1.63(13)	0.73(14)	1.13(13)
N6	0.86(37)	1.59(3)	1.72(17)	2.19(4)	1.72(18)	0.51(8)	1.35(27)

- $M_S \approx 1.0$  GeV : slightly above the experimental result from the Belle Collaboration ( $M_S = 796(54)$  MeV for the isoscalar scalar meson [Masuda '15])
- $M_A \approx 1.4$  GeV to be compared with the experimental value by the L3 Collaboration  $M_A = 1040(80)$  MeV for the isoscalar meson  $f_1(1285)$  [Achard '01, '07].
- $M_T^{(2)} \approx 1.4$  GeV,  $M_{0,T}^{(1)} \approx 1.6$  GeV and  $M_{(1)}^{(0,T)} \approx 2.0$  GeV, above the experimental values for the  $f_2(1270)$  mesons obtained by fitting the single-virtual form factor [Masuda '15, Danilkin '16].